

# The Role of Solvent Viscosity in the Dynamics of Protein Conformational Changes

Anjum Ansari, Colleen M. Jones, Eric R. Henry,  
James Hofrichter, William A. Eaton\*

Nanosecond lasers were used to measure the rate of conformational changes in myoglobin after ligand dissociation at ambient temperatures. At low solvent viscosities the rate is independent of viscosity, but at high viscosities it depends on approximately the inverse first power of the viscosity. Kramers theory for unimolecular rate processes can be used to explain this result if the friction term is modified to include protein as well as solvent friction. The theory and experiment suggest that the dominant factor in markedly reducing the rate of conformational changes in myoglobin at low temperatures (<200 K) is the very high viscosity (>10<sup>7</sup> centipoise) of the glycerol-water solvent. That is, at low temperatures conformational substates may not be "frozen" so much as "stuck."

Important information on the mechanism and dynamics of a molecular process can be obtained by studying the dependence of its kinetics on solvent viscosity. Classic examples are the investigation of the role of diffusion in determining the rate of a bimolecular reaction (1) and the influence of solvent friction on a unimolecular reaction rate (2). Other examples include the effect of solvent viscosity on the motion of small molecules inside proteins (3) and the contribution of diffusive processes to the rate-limiting steps in protein folding (4). Here we show how such studies can be used to gain insight into the dynamics of conformational changes in proteins.

The carbon monoxide complex of myoglobin (MbCO) is dissociated by light. The conformation of the photoproduct is unstable, and the protein relaxes to the conformation of the unliganded molecule by a small but global displacement of protein atoms on one side of the heme. We have investigated the kinetics of this conformational change as a function of solvent viscosity by using high-precision, time-resolved absorption measurements after photodissociation by nanosecond laser pulses. A representative set of time-resolved absorption spectra in a 79% by weight solution of glycerol in water at 20°C is shown in Fig. 1. The time course of the decrease in the overall amplitude of the difference spectra measures the ligand rebinding kinetics, which take place in two phases (Fig. 2A). The first, nonexponential phase, with a half-time of about 200 ns, corresponds to geminate rebinding, that is, unimolecular rebinding of CO to the heme from which it was photodissociated (5). The second phase, at about 1 ms, corresponds to bimolecular rebinding of CO from the solvent.

There are also changes in the shape of the spectra, which are primarily spectral changes of the deoxyheme photoproduct (Fig. 2B). The corresponding amplitudes (Fig. 2, B and C) monitor the extent of the deviations of the observed spectra from the average spectrum shown in Fig. 2A. We interpret these spectral changes as arising from protein conformational changes following photodissociation. Lambright *et al.* (6) have independently observed these kinetics but did not investigate their viscosity dependence.

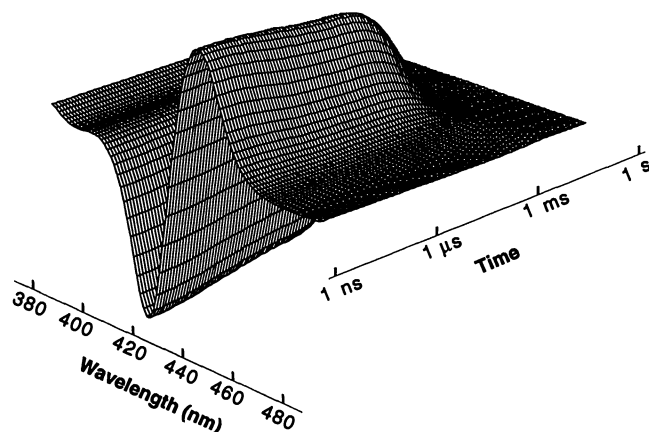
The similarity of the deoxyheme spectral changes to those observed for hemoglobin suggests that they correspond to a displacement of the iron relative to the heme plane that is coupled to a protein conformational change on the proximal side of the heme (7). Comparison of the x-ray structures of Mb and MbCO shows a small global displacement of the protein atoms on the proximal side (8), and this is most likely the

protein conformational change that is being monitored in our experiments. This conformational change is interesting because it could be responsible for slowing down the rate of ligand rebinding to produce the nonexponential geminate phase (9, 10). Its global nature suggests that its rate would be influenced by solvent viscosity. There is also a localized rearrangement of side chains on the distal side of the heme observed in the x-ray studies (8) that may correspond to the 200- to 300-ps process observed in circular dichroism studies (11) or contribute to the sub-30-ps events detected in phase-grating spectroscopic experiments (12).

The data in Fig. 2, B and C, show that there is an initial large-amplitude process in the kinetics of the protein conformational change, which is followed by smaller amplitude processes (13). We shall be concerned here only with the large-amplitude initial process (indicated by the arrows in Fig. 2, B and C), for which relatively precise rate constants can be derived. The major result is that increasing the viscosity increases the amplitude of the initial process that was resolved with our 10-ns laser pulses, which indicates a slowing of the conformational change. Studies by Frauenfelder and co-workers (3) showed that ligand rebinding rates at a given viscosity and temperature are the same for different solvents, which implies that the effect of glycerol on the conformational kinetics in our experiments does not result from a solvent effect other than viscosity.

The data in Fig. 2, B and C, show that the kinetic progress curve for the initial conformational relaxation is at least biexponential. In order to obtain a single rate constant under each set of conditions, we

**Fig. 1.** Time-resolved optical absorption spectra following photodissociation of the CO complex of sperm whale myoglobin. Deoxy-minus-CO difference spectra of photodissociated MbCO in 79% by weight glycerol-water at 20°C are shown as a function of time. The experiments were carried out with the use of two Nd:YAG (yttrium-aluminum-garnet) lasers that produced 10-ns pulses for photolysis and optical absorption measurements as described (21). In order to eliminate effects due to rotational diffusion of the photoselected populations in incompletely photolyzed samples, we obtained isotropically averaged spectra by making measurements with the polarization of the photolysis pulse both parallel to and perpendicular to the polarization of the probe pulse. The rotational correlation time was determined from the decay in the optical anisotropy and exhibited Stokes-Einstein behavior, which indicates that increasing the glycerol concentration has no perceptible effect on either the size or the shape of the protein.



Laboratory of Chemical Physics, Building 2, National Institute of Diabetes and Digestive and Kidney Diseases, National Institutes of Health, Bethesda, MD 20892.

\*To whom correspondence should be addressed.

simultaneously fit 21 kinetic progress curves that were obtained in water, 56% by weight glycerol-water, and 79% by weight glycerol-water between  $-5^{\circ}\text{C}$  and  $+35^{\circ}\text{C}$ , with the use of a stretched exponential function for the initial relaxation (14):

$$A(t) = A_0 \exp(-kt)^{\beta} \quad (1)$$

where it is assumed that  $A_0$ , the amplitude at  $t = 0$ , and  $\beta$  are the same under all conditions. The rate constants  $k$  obtained from these fits for  $\beta = 0.6$  and  $A_0 = 0.06$  are shown in Fig. 3 as a function of the solvent viscosity (15).

The theoretical explanation for the effect of solvent viscosity on unimolecular rate processes in the condensed phase is provided by the Kramers theory (2), which shows that for a diffusive barrier-crossing the rate is inversely proportional to the friction. For protein conformational changes, two sources of friction must be considered because only a fraction of the protein atoms is in contact with solvent atoms. One is the friction of the solvent, which retards the motion of atoms on the surface

of the protein; the other is the internal friction of the protein, which slows the motion of protein atoms relative to each other. If we assume that the friction of the protein and solvent is additive, the Kramers equation (2) for the rate constant in the high-friction limit becomes:

$$k = \frac{B}{\alpha\zeta_p + (1 - \alpha)\zeta_s} \exp(-E_0/RT) \quad (2)$$

where  $R$  is the gas constant,  $T$  is the temperature,  $E_0$  is the average height of the potential energy barrier separating the protein conformations,  $B$  is a viscosity- and temperature-independent parameter that depends on the shape of the potential surface,  $\zeta_p$  is the friction constant for motion in the protein, and  $\zeta_s$  is the friction constant for motion in the solvent which, according to Stokes' law, is proportional to its viscosity. In Eq. 2 the relative contributions of protein and solvent friction are approximated by the parameter  $\alpha$ , which is the fraction of protein atoms involved in the conformational change that are not in

contact with solvent atoms. For simplicity, we ignore any dependence of the protein friction constant on the solvent viscosity or temperature.

To apply Eq. 2 to the experimental data, we write the pre-exponential factor in terms of the known solvent viscosity,  $\eta$ , and the adjustable parameters  $C$  and  $\sigma$ :

$$k = \frac{C}{\sigma + \eta} \exp(-E_0/RT) \quad (3)$$

$\sigma$  has units of viscosity and can be thought of as the contribution of the protein friction to the total friction. The data in Fig. 3 exhibit the characteristic features of this equation, that is, a small viscosity dependence at low solvent viscosities and an inverse first-power viscosity dependence at high solvent viscosities. This result does not depend on the use of the stretched exponential function (Eq. 1) because it is also obtained with  $\beta = 1$  (lower error limits in Fig. 3).

The fit to the data in Fig. 3 with the use of Eq. 3 yields values of  $C = 7.2 \pm 3.0 \times 10^{10} \text{ cP/s}$ ,  $\sigma = 4.1 \pm 1.3 \text{ cP}$ , and  $E_0 = 2.4 \pm 2.2 \text{ kcal/mol}$ . This value for  $\sigma$  suggests that the solvent viscosity coordinate at ambient temperatures may be divided into approximately three regions: (i) below  $\sim 1 \text{ cP}$  (the viscosity of water at  $20^{\circ}\text{C}$ ), where the solvent friction makes a small contribution to decreasing the rate constant for this conformational change; (ii) between 1 and 15 cP, where both the protein friction and the solvent friction contribute to decreasing

**Fig. 2.** Kinetics of ligand rebinding and conformational changes following photodissociation of MbCO. Spectra for different solvent compositions and temperatures of the type shown in Fig. 1 were analyzed with the use of singular value decomposition (SVD), which transforms the data set  $D$  into a product of three matrices:  $D = USV^T$  (22). The columns of  $U$  represent the minimal set of orthonormal basis spectra, the columns of  $V$  are the corresponding amplitudes as a function of time, and the diagonal elements of  $S$  are a measure of the contribution of the corresponding basis spectra to the observed spectra. After correcting for the temperature and solvent dependence of the spectra, the data at all temperatures and viscosities can be represented in terms of two basis spectra. **(A)** Time course of the amplitude of the first basis spectrum in three different solvents at  $20^{\circ}\text{C}$ , in 0.1 M phosphate buffer (pH 7.0) and 10 mM  $\text{Na}_2\text{S}_2\text{O}_4$ . Upper curve, water; middle curve, 56% by weight glycerol-water; lower curve, 79% by weight glycerol-water. The first basis spectrum (shown in the inset) is an average deoxy-minus-CO difference spectrum; the corresponding amplitudes are normalized to 1 at  $t = 0$  and represent a very good approximation to the fraction of deoxyhemes. Differences in the bimolecular rebinding rate at times longer than 100  $\mu\text{s}$  are due in part to differences in the free CO concentration. **(B and C)** Time course of the amplitudes of the second basis spectrum at  $20^{\circ}\text{C}$  (B) and  $5^{\circ}\text{C}$  (C) normalized by the fraction of deoxyhemes. Lower curve, water; middle curve, 56% by weight glycerol-water; upper curve, 79% by weight glycerol-water. The second basis spectrum [shown in the inset to (B)] is primarily a spectral change of the deoxyhemes; the corresponding amplitudes represent the kinetics of the deoxyheme spectral changes, which are interpreted as the kinetics of the protein conformational change on the proximal side of the heme. The continuous curves are the least squares best fit to the data described in (15). The arrows indicate the relaxation times for the initial relaxation described by Eq. 1.

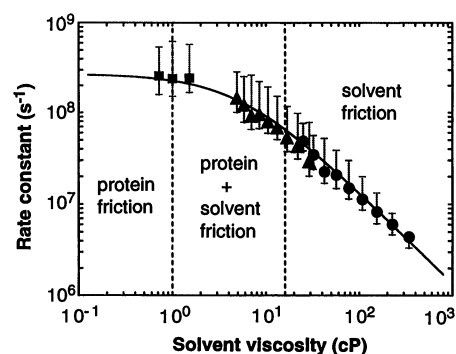
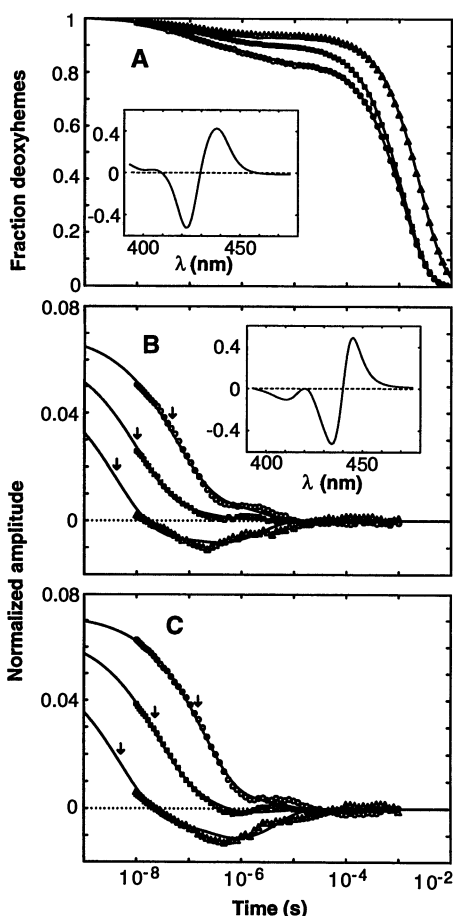


**Fig. 3.** Rate constant for Mb conformational change as a function of solvent viscosity. The plotted values are the rate constants for the initial, large-amplitude process and were obtained by fitting the data with a stretched exponential function (Eq. 1). The best fit was obtained for  $\beta = 0.62$  and  $A_0 = 0.058$ . The temperatures for both the 56% by weight (triangles) and the 79% by weight (circles) glycerol-water solvents were  $-5^{\circ}\text{C}$  to  $+35^{\circ}\text{C}$  at intervals of  $5^{\circ}\text{C}$ , whereas the temperatures for water (squares) were  $5^{\circ}$ ,  $20^{\circ}$ , and  $35^{\circ}\text{C}$ . Fitting these rate constants with Eq. 3 shows that the activation energy is small ( $E_0 = 2.4 \pm 2.2 \text{ kcal/mol}$ ), so that most of the change in the rate constant is due to the change in viscosity (15).

the rate constant; and (iii) above 15 cP, where the solvent friction dominates. Extrapolation of these results to low temperatures indicates that solvent viscosity could have very large effects on the rate of conformational change. At  $-95^{\circ}\text{C}$  in 79% by weight glycerol-water, the pre-exponential factor in Eq. 3 for this conformational change is predicted from the viscosity (16) to be reduced by a factor of about  $10^{11}$  compared to the value at  $20^{\circ}\text{C}$ , whereas the exponential term is predicted to be reduced by a factor of less than 200. This extrapolation suggests that the marked decrease in the rate of interconversion of conformational substates at temperatures near the glass transition (10, 17, 18) results more from the enormous viscosity of the solvent than from potential energy barriers that are large compared to the average thermal energy. That is, at low temperatures conformational substates may not be "frozen" so much as "stuck." This hypothesis predicts that the low-temperature kinetics of Mb, which has a broad distribution of ligand rebinding rates resulting from a distribution of noninterconverting conformational substates (10, 17), would be mimicked at room temperature in very high viscosity solvents. Distributed kinetics at room temperature have, in fact, been observed in solid polyvinyl alcohol (17).

What is the influence of solvent viscosity on the rate of protein conformational changes under physiological conditions? The viscosity of cytoplasm has been estimated to be about 2 to 3 cP (19). Although we do not yet know anything about the values of  $\sigma$  for other proteins, the present results suggest that intracellular viscosities could slow protein conformational changes significantly and therefore influence the kinetics of protein function (20).

## REFERENCES AND NOTES

1. M. Smoluchowski, *Z. Phys. Chem.* **92**, 129 (1917); S. A. Rice, *Diffusion-Limited Reactions*, vol. 25 of *Comprehensive Chemical Kinetics* (Elsevier, Amsterdam, 1985).
2. H. A. Kramers, *Physica (Utrecht)* **7**, 284 (1940); P. Hänggi, P. Talkner, M. Borkovec, *Rev. Mod. Phys.* **62**, 251 (1990).
3. D. Beece *et al.*, *Biochemistry* **19**, 5147 (1980).
4. B. A. Chrunyk and C. R. Matthews, *ibid.* **29**, 2149 (1990).
5. E. R. Henry, J. H. Sommer, J. Hofrichter, W. A. Eaton, *J. Mol. Biol.* **166**, 443 (1983); A. Ansari *et al.*, *Biochemistry* **25**, 3139 (1986).
6. D. G. Lambright, S. Balasubramanian, S. G. Boxer, *Chem. Phys.* **158**, 249 (1991).
7. L. P. Murray, E. R. Henry, J. Hofrichter, W. A. Eaton, *Biophys. Chem.* **29**, 63 (1988).
8. J. Kuriyan, S. Wilz, M. Karplus, G. A. Petsko, *J. Mol. Biol.* **192**, 133 (1986).
9. N. Agmon and J. J. Hopfield, *J. Chem. Phys.* **79**, 2042 (1983); E. R. Henry, J. Hofrichter, J. H. Sommer, W. A. Eaton, in *Brussels Hemoglobin Symposium*, A. G. Schnek and C. Paul, Eds. (Edition de l'Université de Bruxelles, Brussels, 1983), pp. 193–203; J. Hofrichter *et al.*, *Biochemistry* **24**, 2667 (1985).
10. P. J. Steinbach *et al.*, *Biochemistry* **30**, 3988 (1991).

11. X. Xie and J. D. Simon, *ibid.*, p. 3682.
12. L. Genberg, L. Richard, G. McLendon, R. J. D. Miller, *Science* **251**, 1051 (1991).
13. One of the smaller amplitude relaxations may correspond to the 700-ns process observed in water at  $20^{\circ}\text{C}$  by photoacoustic calorimetry [J. A. Westrick, J. L. Goodman, K. S. Peters, *Biochemistry* **26**, 8313 (1987)].
14. H. Frauenfelder *et al.*, *J. Phys. Chem.* **94**, 1024 (1990); H. Frauenfelder, S. G. Sligar, P. G. Wolynes, *Science* **254**, 1598 (1991).
15. The rate constants shown were corrected for the activation energy to the reference temperature of  $20^{\circ}\text{C}$ . The viscosities were calculated from the empirical function of Hasinoff (23). The rate constants were obtained in a three-step procedure designed to remove the contribution of the slower, smaller amplitude processes. First, we obtained a set of rate constants, parameterized by Eq. 3, by simultaneously fitting both the ligand rebinding curves ( $V_1$ ) and the unnormalized progress curves ( $V_2$ ) for the deoxyheme spectral changes to a sum of four relaxations (22). In this fit a stretched exponential was used to describe the first relaxation, exponentials to describe the next two relaxations, and the integrated form of the second-order rate equation to describe the final bimolecular relaxation. Second, the contribution of the bimolecular relaxation was subtracted from the progress curves for the deoxyheme spectral changes, and these curves were normalized to 100% deoxyhemes with the use of the ligand rebinding curves (Fig. 2A). Finally, we refit the normalized data for the deoxyheme spectral changes (Fig. 2, B and C) by using Eq. 1 for the first process with a single value of  $\beta$  and by allowing the rate constant to be optimized independently for each progress curve. In this fit the amplitude of the first relaxation was constrained to be independent of both solvent and temperature, the rates for the two slower processes were constrained to the values obtained in the simultaneous fit with the ligand rebinding curves, and the
16. A. A. Newman, *Glycerol* (CRC Press, Cleveland, 1968); D. H. Rasmussen and A. P. MacKenzie, *J. Phys. Chem.* **75**, 967 (1971); C. A. Angell and W. Sichina, *Ann. N.Y. Acad. Sci.* **279**, 53 (1976).
17. R. H. Austin, K. W. Beeson, L. Eisenstein, H. Frauenfelder, I. C. Gunsalus, *Biochemistry* **14**, 5355 (1975).
18. A. Ansari *et al.*, *Biophys. Chem.* **26**, 337 (1987); I. E. T. Iben *et al.*, *Phys. Rev. Lett.* **62**, 1916 (1989); V. Šrajer, L. Reinisch, P. M. Champion, *Biochemistry* **30**, 4886 (1991).
19. A. M. Mastro and A. D. Keith, *J. Cell Biol.* **99** (part 2), 180s (1984).
20. B. Gavish and M. M. Werber, *Biochemistry* **18**, 1269 (1979); A. P. Demchenko, O. I. Rusyn, E. A. Saburova, *Biochim. Biophys. Acta* **998**, 196 (1989).
21. J. Hofrichter *et al.*, *Biochemistry* **30**, 6583 (1991).
22. J. Hofrichter, J. H. Sommer, E. R. Henry, W. A. Eaton, *Proc. Natl. Acad. Sci. U.S.A.* **80**, 2235 (1983); E. R. Henry and J. Hofrichter, *Methods Enzymol.* **210**, 129 (1992).
23. B. B. Hasinoff, *Arch. Biochem. Biophys.* **183**, 176 (1977).
24. We thank B. Bagchi, M. Edidin, F. Stillinger, A. Szabo, and R. Zwanzig for helpful discussions.

27 February 1992; accepted 14 April 1992

## Probing Protein Stability with Unnatural Amino Acids

David Mendel, Jonathan A. Ellman, Zhiyuh Chang,  
David L. Veenstra, Peter A. Kollman, Peter G. Schultz\*

Unnatural amino acid mutagenesis, in combination with molecular modeling and simulation techniques, was used to probe the effect of side chain structure on protein stability. Specific replacements at position 133 in T4 lysozyme included (i) leucine (wt), norvaline, ethylglycine, and alanine to measure the cost of stepwise removal of methyl groups from the hydrophobic core, (ii) norvaline and *O*-methyl serine to evaluate the effects of side chain solvation, and (iii) leucine, *S*,*S*-2-amino-4-methylhexanoic acid, and *S*-2-amino-3-cyclopentylpropanoic acid to measure the influence of packing density and side chain conformational entropy on protein stability. All of these factors (hydrophobicity, packing, conformational entropy, and cavity formation) significantly influence protein stability and must be considered when analyzing any structural change to proteins.

Mutational studies of the amino acids that form the hydrophobic core of proteins are beginning to define how these residues influence protein structure and stability (1–10). However, it is difficult to make mutations with the natural 20 amino acids that perturb one interaction without simultaneously affecting several others. For example, mutation of Leu<sup>133</sup> → Phe or Ala<sup>129</sup> → Val in T4 lysozyme (T4L) in an attempt to

increase packing density, and as a consequence, thermal stability, resulted in a less

D. Mendel, J. A. Ellman, Z. Chang, P. G. Schultz, Department of Chemistry, University of California, Berkeley, Berkeley, CA 94720, and Center for Advanced Materials, Lawrence Berkeley Laboratory, Berkeley, CA 94720.

D. L. Veenstra and P. A. Kollman, Department of Pharmaceutical Chemistry, University of California, San Francisco, San Francisco, CA 94143.

\*To whom correspondence should be addressed.